PERGAMON

International Journal of Solids and Structures 40 (2003) 729–745

INTERNATIONAL JOURNAL OF SOLIDS and STRUCTURES

www.elsevier.com/locate/ijsolstr

Stress-driven morphological instability and catastrophic failure of microdevices

Paolo Decuzzi *, Giuseppe P. Demelio

Center of Excellence in Computational Mechanics (CEMeC), Dipartimento di Ingegneria Meccanica e Gestionale, Politecnico di Bari, Viale Japigia, 182, 70126 Bari, Italy

Received 20 November 2001; received in revised form 30 September 2002

Abstract

In microdevices, the competition between surface energy and elastic energy could lead at the phenomenon known as stress-driven morphological instability (MI), causing an increase of surface roughness with time. Several different mass transport mechanisms can trigger such a morphological alteration and operate simultaneously: surface and bulk diffusion, evaporation and condensation, chemical reactions. Unstable solids could eventually evolve towards crack-like surfaces thus altering mechanical, electrical and optical properties of the devices or even leading to catastrophic failures by supercritical crack propagation. In this work, a more general kinetic law is employed to estimate the onset of MI, considering the effect of the stress field on the atomic mobility. A more intuitive and straightforward approach is used to determine the stability conditions, where the rate of atomic mass motion is introduced as a stability parameter. The critical loads and wavelengths for the onset of MI, determined as a function of material parameters α and β, are compared with the limiting conditions for the supercritical crack propagation (SC) of a crack-like surface in order to asses if and under which situations catastrophic failures by SC can be observed. Two practical cases are investigated: fixed wavelength (Case I) and arbitrary rough surface with a fixed remote load (Case II). In Case I, absolute and relative threshold loads are found below which MI could never occur and a transitional wavelength over which MI would always lead to SC is introduced. In Case II, it is shown that dominant perturbation for MI would always lead to SC given enough time for the surface to evolve towards a crack-like profile. The influence of the material properties α and β on the critical parameters is also addressed.

Keywords: Instability; Failure; Propagation

1. Introduction

It is well known that surface morphology can be altered by atomic mass transport due to bulk and surface diffusion, evaporation and condensation, and chemical reactions. Thermal gradients, mechanical stresses, electrical and magnetic fields, ion or photon bombardment can modify the surface free energy of

* Corresponding author. Tel.: +39-80-59-62-718; fax: +39-80-59-62-777.
E-mail address: p.decuzzi@poliba.it (P. Decuzzi).

0020-7683/02/$ - see front matter © 2002 Elsevier Science Ltd. All rights reserved.
PII: S0020-7683(02)00610-8

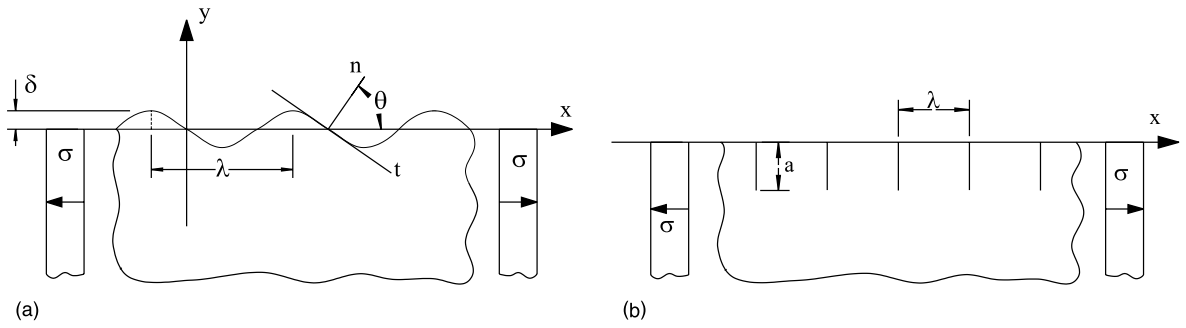

Fig. 1. (a) The perturbed surface profile of an elastic half-plane loaded by a remote uniform stress σ_∞: λ and δ are respectively the wavelength and the semi-amplitude of the perturbation. (b) A 'crack-like surface' is an array of edge cracks with spacing λ and depth a loaded remotely by an uniaxial load σ_∞.

solids thus triggering mass transport. Stability and control of surfaces' evolution are issues of great interest in microdevices, where even slight corrugations can alter mechanical, electrical and optical performances, and in thin fragile ceramic films where static fatigue can occur.

Consider a solid under remote uniaxial loading σ_∞ with a non-planar surface (Fig. 1a). The stress field below the interface is not uniform and the elastic energy stored at the valleys is larger than the unperturbed value $w_\infty(\propto \sigma_\infty^2/E)$, whilst the elastic energy stored at the crests is smaller than the unperturbed value. On the other hand, the surface energy being proportional to the surface curvature is non-uniform and it is positive at the crests and negative at the valleys. Consequently, the free energy of the surface defined as the sum of the elastic strain energy, surface energy and chemical energy, is not uniform. With such a scenario, since atoms migrate spontaneously from sites of larger free energy towards sites of smaller free energy, morphological alterations are expected. Considering surface diffusion as the mechanism for atomic mass transport, the elastic energy pushes atoms from the valleys towards the crests, thus increasing the profile roughness, whereas the surface energy pushes atoms in the opposite direction. Similarly, if chemical reactions take place at the free surface and the solid looses mass, the surplus of elastic energy at the valleys pushes atoms away from the solid to the parent phase, usually a fluid, whilst again the surface energy has the opposite effect pushing atoms away from the crests. Therefore, if the effect of surface energy is larger than the contribution of elastic energy the system would be stable and the initial roughness flattened; conversely, if the effect of the elastic energy is larger than the contribution of the surface energy the system would be unstable and the initial roughness would grow with time. This instability related to the competition between elastic and surface energies is also known as *energetically driven morphological instability* (MI), and has been identified by Asaro and Tiller (1972) for stress corrosion cracking.

Such a phenomenon has been recently the object of several studies. For instance, Srolovitz (1989) has determined a critical wavelength of the initial surface roughness above which the system is always unstable given by

$$\lambda_{\mathrm{cr}} = \frac{\pi E \gamma}{(1-\nu^2)\sigma_\infty^2} \tag{1}$$

for an elastic half-plane under uniaxial remote loading, where γ is the surface tension, E and ν are the Young's modulus and Poisson's ratio respectively. The calculations of Srolovitz were conducted under the assumption of stress independent surface diffusivity D_s and atoms mobility M. In 1991, Aziz and coworkers have firstly showed and measured the influence of the stress field on atomic surface mobility introducing the concept of activation strain tensor V_{ij}^*. Subsequently, it has been shown that such stress-dependence can affect surface stability and cause the so called *kinetically driven MI* (Barvosa-Carter et al., 1998).

The above mentioned analysis are devoted to the estimation of the onset of MI and are based on small perturbation techniques. Therefore they cannot be employed to study the long-term evolution of surface profiles. This can be only done by means of numerical analysis as those performed by Yang and Srolovitz (1993), Chiu and Gao (1994) and Freund (1995). In the first two papers, the evolution of wavy profiles due to surface diffusion has been studied showing that an initially unstable profile ($\lambda > \lambda_{cr}$) evolves over time towards a flawed surface which can be assimilated to an array of edge cracks with spacing λ. Yang and Srolovitz have written of evolution towards a *crack-like surface*, whilst Chiu and Gao have referred to a *cuspidal profile*. In addition, more recently, Yu and Suo (1999) have studied the nucleation and subsequent propagation of cracks on the free surface of polycrystalline materials exposed to corrosive environment, where the dominating atomic mass transport are evaporation, condensation and chemical reactions. They have again shown that the initial wavy surface can evolve towards a crack-like interface. They also estimated a normalized threshold parameter Λ_{th} above which the nominally flat surface is unstable and a crack front can nucleate

$$\Lambda_{th} = \left(\frac{\sigma^2\lambda}{E\gamma_s}\right)_{th} = 4 - 2\frac{\gamma_B}{\gamma_S} \tag{2}$$

where γ_S and γ_B are the surface energies per unit length at the free surface and grain boundary respectively.

The discussion so far conducted has shown that three stages can be depicted during the life of a surface susceptible to MI: (i) initiation of MI; (ii) evolution of the surface profile towards a flawed surface with spacing λ ($\geqslant \lambda_{cr}$); (iii) supercritical propagation of surface flaws and catastrophic failure. In this work, attention is focused on stages (i) and (iii) with the aim of determining the critical conditions (critical wavelength and critical stress) for the onset of MI and the limiting conditions for the supercritical propagation of surface flaws (SC). The dependence of the atomic mobility on the stress field is considered as from Barvosa-Carter et al. (1998). Thus the critical conditions for MI are compared with those for SC for understanding if and under which conditions MI could lead to catastrophic failure, as a function of the material properties.

2. Stress-driven morphological instability

An elastic half-plane with a nominally flat surface loaded by an uniaxial uniform stress σ_∞ is considered, as from Fig. 1a. The critical conditions for the onset of the stress-driven MI are determined by means of a small perturbation analysis. Therefore, the nominally flat surface is perturbed by a sinusoidal profile $h(x) = \delta e^{jmx}$, where δ is the semi-amplitude and $m = 2\pi/\lambda$ the wave number of the perturbation. Under the hypothesis of small perturbations, i.e. $h'(x) \propto \delta m \ll 1$, any perturbed physical quantity q can be expressed as $q = q(y)e^{jmx}$.

2.1. The perturbed stress field

The governing equation for a linear elasticity problem in terms of the displacement vector $\mathbf{u} = u\mathbf{i} + v\mathbf{j} + w\mathbf{k}$ is given by

$$\nabla div\mathbf{u} + (1-2\nu)\nabla^2\mathbf{u} = \mathbf{0} \tag{3}$$

Thus, introducing the perturbed components of the stress field $u = u(y)e^{jmx}$, $v = v(y)e^{jmx}$ and $w = w(y)e^{jmx}$, and imposing the boundary conditions at infinity ($\mathbf{u} \to \mathbf{0}$ for $y \to -\infty$), it follows after some algebra that

$$u(x,y) = [A_1 + A_2 y]\mathrm{e}^{my}\mathrm{e}^{jmx}$$
$$v(x,y) = j\left[\left(\frac{(3-4\nu)}{m}A_2 - A_1\right) - A_2 y\right]\mathrm{e}^{my}\mathrm{e}^{jmx} \tag{4}$$

where the constants A_1 and A_2 must be determined imposing the boundary conditions at the free surface $h(x)$: normal tractions $\sigma_{\mathrm{nn}}(x)$ and tangential tractions $\sigma_{\mathrm{tn}}(x)$ are zero (more details are given in Srolovitz, 1989). Recalling the well known compatibility and constitutive equations of the linear theory of elasticity, it follows that

$$A_1 = 2j\frac{(1-\nu)}{2\mu}\delta\sigma_\infty; \quad A_2 = j\frac{\sigma_\infty}{2\mu}(m\delta) \tag{5}$$

where higher order terms have been neglected ($\mathrm{O}[(m\delta)^2\mathrm{e}^{j2mx}] \approx 0$). Finally, the perturbed stress field has the form

$$\sigma_{xx}(x,y) = -\sigma_\infty(m\delta)[2+my]\mathrm{e}^{my}\mathrm{e}^{jmx}$$
$$\sigma_{yy}(x,y) = \sigma_\infty(m\delta)[my]\mathrm{e}^{my}\mathrm{e}^{jmx} \tag{6}$$
$$\sigma_{xy}(x,y) = j\sigma_\infty(m\delta)[1+my]\mathrm{e}^{my}\mathrm{e}^{jmx}$$

and the strain energy density on the surface, under plane strain conditions $\sigma_{zz} = \nu(\sigma_{xx} + \sigma_{yy})$, is given by

$$w - w_\infty = -2\frac{(1-\nu^2)}{E}\sigma_\infty^2(m\delta)\mathrm{e}^{jmx} \tag{7}$$

where $w_\infty = (1-\nu^2)\sigma_\infty^2/2E$ is the unperturbed contribution.

2.2. The kinetic law

It is well known that atoms are in continuous 'chaotic' motion and in the absence of any external driving force (thermal gradients, surface and chemical energy gradients, electrical and magnetic fields, gravitational and stress fields, and ion/photon bombardment) every particles has the same probability of moving in any direction independently from its original position, in an isotropic and infinite solid or fluid. Macroscopic mass transport, and consequently morphological alterations, are due to the ordered motion of atoms, independently of the transport mechanism which can be either surface and bulk diffusion, evaporation and condensation, chemical reactions.

The rate r at which atoms move is related to the intensity of driving forces pushing the atoms to migrate from the more energetic site 1 to the less energetic site 2. Assuming that the imposition of external fields leads to a reduction of the free energy in site 2 relative to site 1 by an amount of $2\Delta G$, following Ohring (1992, Section 1.6.2), the rate r can be written as

$$r_{1\rightleftarrows 2} = \nu\exp\left[-\frac{G^* \mp \Delta G}{kT}\right] \tag{8}$$

where $k = 1.3806568 \times 10^{-23}\ \mathrm{J\,K^{-1}}$ is the Boltzman constant, ν is the characteristic lattice frequency, G^* is the Gibbs free energy of activation for the assumed mass transport mechanism and T is the absolute temperature. The rate $r_{1\to 2}$ can be interpreted as the number of atoms per second moving from 1 to 2. From (8), a positive net rate of atoms from 1 to 2 is derived as

$$r = [r_{1\to 2} - r_{2\to 1}] \propto \exp\left[-\frac{G^*}{kT}\right]\sinh\left(-\frac{\Delta G}{kT}\right) \tag{9}$$

In (9), the first term is related to the activation energy G^* and it is proportional to the atomic mobility M; whilst the second term is related to the driving force F of the system, defined as $F = -\Delta G > 0$ for spontaneous evolutions. In the most general form G^* can be written as the sum of the activation energy for the stress-free state Q^*, the strain activation energy $V^*_{ij}\sigma_{ij}$ and the surface activation energy $\gamma^*_{ij}\kappa_{ij}$, that is

$$G^* = Q^* - V^*_{ij}\sigma_{ij} - \gamma^*_{ij}\kappa_{ij} \tag{10}$$

Usually, the contribution of $\gamma^*_{ij}\kappa_{ij}$ could be neglected, and it is not considered in the sequel. Whereas, the free energy variation ΔG is given by the sum of the contributions of the chemical energy ΔG_0, surface energy $\Delta G_\kappa = \gamma_{ij}\kappa_{ij}$ and elastic energy ΔG_σ, that is

$$\Delta G = \Delta G_0 + \Delta G_\kappa + \Delta G_\sigma = -F \tag{11}$$

Notice that the above relations are general in that they are independent of the mass transport mechanism. Moreover, the effect of the stress field on the activation energy G^*, or atomic mobility M, is considered introducing the strain activation energy tensor V^*_{ij}, defined as

$$V^*_{ij} = kT\frac{\partial \log M}{\partial \sigma_{ij}} \tag{12}$$

by Aziz et al. (1991).

2.3. Stability of the surface and characteristic equation

Morphological alterations of the surface are due to atomic mass transport. It is then natural to relate the stability analysis of the surface to the stability of atomic motion and introduce the variation of the net rate of atomic motion r with the perturbation as a stability parameter. An infinitesimal increase $\mathrm{d}h$ in surface profile amplitude causes a perturbation $\mathrm{d}r$ of the rate at which atoms move: (i) for $\mathrm{d}r/\mathrm{d}h < 0$ a perturbation of the surface profile leads to a negative rate of atomic motion, that is to say the atomic motion opposes the perturbation of the surface reducing its amplitude with time (*stable perturbation*); (ii) for $\mathrm{d}r/\mathrm{d}h > 0$ a perturbation of the surface profile leads to a positive rate of atomic motion, that is to say the atomic motion favors the evolution of the surface whose amplitude grows indefinitely with time (*unstable perturbation*); the onset of instability is then given by (iii) $\mathrm{d}r/\mathrm{d}h = 0$, for which the amplitude of the perturbed profile neither grows nor decays (*threshold condition*).

It is thus clear that the stability of the system is assessed regardless of the atomic mass transport mechanism, which could be diffusion, evaporation and condensation, chemical reactions.

From (9), the stability parameter $\mathrm{d}r/\mathrm{d}h$ can be estimated and after straightforward algebraic calculations it results

$$\frac{\mathrm{d}r}{\mathrm{d}h} \propto \exp\left(\frac{-G^*}{kT}\right)\cosh\left(\frac{-\Delta G}{kT}\right)\left\{\tanh\left(\frac{\Delta G}{kT}\right)\frac{\mathrm{d}}{\mathrm{d}h}\left[\frac{G^*}{kT}\right] - \frac{\mathrm{d}}{\mathrm{d}h}\left[\frac{\Delta G}{kT}\right]\right\} \tag{13}$$

Observing that the term $[\exp(-G^*/kT)\cosh(-\Delta G/kT)]$ is always positive, and substituting the expressions for G^* and ΔG reported in (10) and (11) respectively, the stability of the system is assessed by checking the sign of the following characteristic equation

$$2\tanh\left[\frac{F_0\Omega}{2kT}\right]\frac{\mathrm{d}}{\mathrm{d}h}\left(\frac{V^*_{ij}\sigma_{ij}}{\Omega}\right) - \frac{\mathrm{d}(\gamma\kappa)}{\mathrm{d}h} - \frac{\mathrm{d}w}{\mathrm{d}h} \gtrless 0 \tag{14}$$

(i) a positive value of the characteristic equation means an unstable system ($dr/dh > 0$); (ii) a negative value of the characteristic equation means a stable system ($dr/dh < 0$); and (iii) a zero value gives the threshold of instability ($dr/dh = 0$). [1]

From (7), the variation of the elastic energy with the amplitude perturbation h can be readily calculated as

$$\frac{dw}{dh} = -2m\frac{(1-\nu^2)}{E}\sigma_\infty^2 < 0 \tag{16}$$

which shows that the effect of the elastic energy is destabilizing and proportional to the wave number m and to the second power of the remote stress σ_∞.

Under the hypothesis of isotropy, the contribution of the surface energy is proportional to the surface curvature $\kappa \approx +m^2 h$ (to the leading order in h), thus

$$\frac{d(\gamma\kappa)}{dh} = +m^2\gamma \tag{17}$$

from which it can be concluded that the effect of the surface energy is stabilizing and is proportional to the second power of the wave number m.

Under the hypothesis of isotropy and symmetry, the components of the activation strain tensor V_{ij}^* in the (x,z)-plane of corrugation are identical $V_{xx}^* = V_{zz}^* = V^*$, whilst the non-symmetric components are zero $V_{ij}^* = 0$. Thus from (6), the contribution of the strain activation energy results as

$$V_{ij}^*\sigma_{ij} = V^*\sigma_\infty(1+\nu)(1-2mh) \tag{18}$$

where the sole stress σ_{xx} gives a non zero contribution. Thus

$$\frac{d}{dh}\left(\frac{V_{ij}^*}{\Omega}\sigma_{ij}\right) = -2(1+\nu)m\frac{V^*}{\Omega}\sigma_\infty \tag{19}$$

from which it derives that for $V^*\sigma_\infty > 0$ the effect of the perturbed surface stress field is stabilizing being $d(V_{ij}^*\sigma_{ij})/dh < 0$, thus increasing the value of (14), whilst for $V^*\sigma_\infty < 0$ the effect of the perturbed surface stress field is destabilizing being $d(V_{ij}^*\sigma_{ij})/dh > 0$, thus increasing the value of (14). The contribution of the activation strain energy is proportional to the wave number m and to the first power of the remote stress σ_∞. Differently from the contribution of the elastic energy, in this case the sign of the remote load influences the stability of the system: for a positive V^*, the system is destabilized by a compressive remote load ($V^*\sigma_\infty < 0$) and stabilized by a tensile remote load ($V^*\sigma_\infty > 0$).

Substituting the relations (16), (17) and (19) in the characteristic equation (14), the stability conditions is obtained as a function of the material properties, remote stress σ_∞ and wave number m.

$$-4\tanh\left[\frac{F_0\Omega}{2kT}\right](1+\nu)\frac{V^*}{\Omega}m\sigma_\infty + 2m\frac{(1-\nu^2)}{E}\sigma_\infty^2 - m^2\gamma \lessgtr 0 \tag{20}$$

This relation is general holding independently of the atomic mass transport mechanism, and it coincides with that given by Yu and Suo (2000) for surface chemical etching, and in the limit of small driving forces

[1] Note that if the free activation energy is independent of the stress field ($V_{ij}^* = 0$), the instability is governed by the sole surface and elastic energies

$$-\frac{d(\gamma\kappa)}{dh} - \frac{dw}{dh} \gtrless 0 \tag{15}$$

The well known energetically driven MI is recovered.

($F_0\Omega/2kT \ll 1$) and activation strain energies ($\sigma_{ij}V^*_{ij}/kT \ll 1$) tends to the stability condition proposed by Voorhess and Aziz (2000). Introducing the material parameters α and β defined as

$$\alpha = \tanh\left[\frac{F_0\Omega}{2kT}\right]\frac{V^*}{\Omega}; \quad \beta = \frac{\pi(1-\nu)}{(1+\nu)}\frac{\gamma}{E} \tag{21}$$

and normalizing the stress as $\breve{\sigma}_\infty = \sigma_\infty(1-\nu)/E$, the characteristic equation (20) can be rephrased in dimensionless form as

$$-4\alpha m\breve{\sigma}_\infty + 2m\breve{\sigma}^2_\infty - m^2\frac{\beta}{\pi} \lessgtr 0 \tag{22}$$

Notice that comparing (15) and (20), it derives that MI can be generally expressed as the superposition of an energetically driven instability (AT) and a kinetically driven instability (BC). The parameter α modulates the prevalence of the AT on BC instability.

2.4. The critical conditions for morphological instability

In the sequel the critical conditions for the onset of MI are analyzed as a function of the material parameters α and β, for two different cases: a fixed wavelength λ of the surface perturbation (Case I) and an arbitrary rough surface with a fixed remote load σ_∞ (Case II).

2.4.1. Case I: Fixed wavelength $\lambda = 2\pi/m$

The characteristic equation (22) is quadratic in the remote stress σ_∞ and the variation of the normalized stability parameter dr/dh against the dimensionless stress $\breve{\sigma}_\infty$ is shown in Fig. 2, for $m = 1$ (m^{-1}) and $\beta = \pi$ (m), and different values of α, namely $\alpha = 0.0$, 1.0, 4.0 and 8.0. Each curve divides the plane in two zones: stable zone where $dr/dh < 0$ and unstable zone where $dr/dh > 0$. Two critical loads can be depicted for $dr/dh = 0$, one is a compressive stress $\breve{\sigma}_{2cr}$ and the other a tensile stress $\breve{\sigma}_{1cr}$, given by

$$\breve{\sigma}_{1cr} = \alpha + \sqrt{\alpha^2 + \frac{\beta}{\lambda}} > 0 \quad \text{and} \quad \breve{\sigma}_{2cr} = \alpha - \sqrt{\alpha^2 + \frac{\beta}{\lambda}} < 0 \tag{23}$$

for $\alpha > 0$. The system is stable for a given wavelength if the remote load is bracketed between the two critical loads, that is

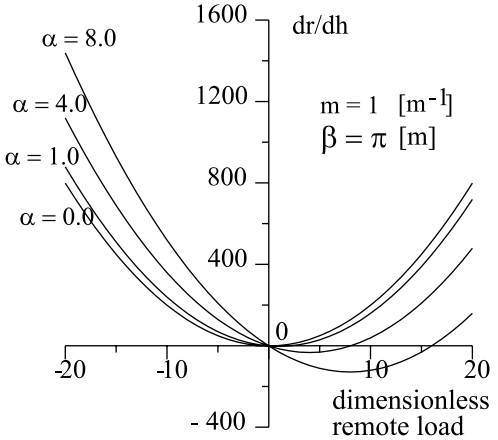

Fig. 2. The stability parameter dr/dh as a function of the dimensionless remote load for different values of the material parameter $\alpha = 0.0$, 1.0, 4.0 and 8.0 ($\beta = \pi$ (m) and $m = 1$ (m^{-1})).

$\sigma > \sigma_{1cr}$ and $\sigma < \sigma_{2cr}$ unstable

$\sigma_{2cr} < \sigma < \sigma_{1cr}$ stable

For a fixed m, the relation (22) gives a parabola $\mathrm{d}r/\mathrm{d}h(\breve{\sigma}_\infty)$

$$\frac{\mathrm{d}r}{\mathrm{d}h} \propto 2m\breve{\sigma}_\infty^2 - 4\alpha m\breve{\sigma}_\infty - m^2\frac{\beta}{\pi} \tag{24}$$

whose vertex is in $(\alpha, -2m\alpha^2 - m^2\beta/\pi)$ and intersects the vertical axes at $-m^2\beta/\pi$. Consequently, as the material parameter α grows the stable area becomes larger and the influence of the sign of the remote load becomes larger too: the tensile critical load grows indefinitely with α whilst the compressive critical load tends to zero. With similar reasonings, opposite conclusions can be drawn in the case of $\alpha < 0$.

For $V^* = 0$, that is $\alpha = 0$, the energetically driven instability is recovered with $\breve{\sigma}_{cr} = \pm\sqrt{\beta/\lambda}$ and the problem is symmetric with respect to $\sigma = 0$ demonstrating that there is no influence of the sign of the remote load on the solution.

2.4.2. Case II: Arbitrary rough surface with a fixed remote load σ_∞

The characteristic equation (22) is quadratic in m, and the variation of the stability parameter $\mathrm{d}r/\mathrm{d}h$ against m is shown in Fig. 3, for $\breve{\sigma}_\infty = \pm 5; \alpha = 1.0$ and $\beta = \pi$ (m). Two different curves are considered depending on the sign of the remote stress. In both cases a critical wave number m_{cr} is depicted above which the perturbation is always unstable. In addition, there is a wave number for which the stability parameter has an absolute maximum m_{max}: this is the dominant perturbation, that is to say a preferred periodicity with wave number m_{max} grows faster than others unstable perturbations. From the relation $\mathrm{d}r/\mathrm{d}h = 0$, the critical wave number can be readily determined as

$$m_{cr} = 2\pi\breve{\sigma}_\infty\frac{\breve{\sigma}_\infty - 2\alpha}{\beta} \tag{25}$$

The wave number of the dominant perturbation is given by $m_{max} = 2m_{cr}$. Correspondingly, a critical wavelength λ_{cr} and dominant wavelength λ_{max} can be defined as

$$\lambda_{cr} = \frac{2\pi}{m_{cr}} = \frac{\beta}{\breve{\sigma}_\infty\left(\breve{\sigma}_\infty - 2\alpha\right)}; \quad \lambda_{max} = \frac{2\pi}{m_{max}} = 2\lambda_{cr} \tag{26}$$

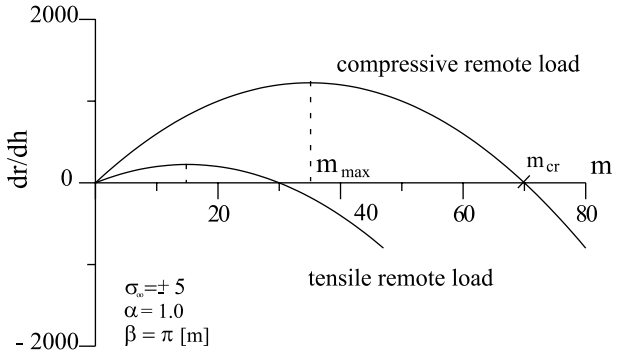

Fig. 3. The stability parameter $\mathrm{d}r/\mathrm{d}h$ as a function of the wave number of the perturbation under tensile and compressive remote load $\sigma_\infty = \pm 5$ ($\alpha = 1.0$, $\beta = \pi$ (m)).

Therefore the stability conditions can be summarized as

$\lambda < \lambda_{cr}$ stable perturbation
$\lambda > \lambda_{cr}$ unstable perturbation
$\lambda = \lambda_{cr}$ dominant perturbation

For $\alpha = 0$, relation (1) is recovered. For a positive α, the largest critical wave number is calculated for a compressive remote load being

$$m_{cr}|_{compression} = 2\pi\breve{\sigma}_\infty \frac{\breve{\sigma}_\infty + 2\alpha}{\beta} > 2\pi\breve{\sigma}_\infty \frac{\breve{\sigma}_\infty - 2\alpha}{\beta} = m_{cr}|_{tension} \tag{27}$$

where the positive value of $\breve{\sigma}_\infty$ is considered in the above relations. Consequently, $\lambda_{cr}|_{compression} < \lambda_{cr}|_{tension}$: for a compressive remote load the range of instability $[\lambda_{cr}, \infty]$ is larger than for a tensile load.

From (25), it can also be concluded that a threshold load exists below which the system is unconditionally stable and MI never occurs. In fact, for $m_{cr} = 0$ instability occurs only for infinitely large wavelengths, therefore the threshold remote load is given by

$$(\breve{\sigma}_\infty)_{th} = 2\alpha = 2\tanh\left[\frac{F\Omega}{2kT}\right]\frac{V^*}{\Omega} \tag{28}$$

Notice that such a threshold load is zero for a compressive load, meaning that in such a case there is no a threshold load. Compressive loading is again the most critical condition, for $\alpha > 0$. By similar reasonings, opposite conclusions can be drawn for a negative α.

3. Stability of an array of edge cracks

Employing large perturbation analysis, Yang and Srolovitz (1993), Chiu and Gao (1994) and Yu and Suo (1999) have shown that initially perturbed surfaces might evolves towards crack-like profiles with spacing λ coinciding with that of the initial perturbation. Notice that, Chiu and Gao (1993) have verified that the intensification of the stress field at the cusp of a cycloid is identical to that of an edge crack under remote tension. Therefore, such profiles can be considered as arrays of edge cracks with spacing λ, as depicted in Fig. 1b. Classical linear fracture mechanics gives the instruments to check whether such cracks can propagate supercritically leading to the catastrophic failure of the device: if the stress intensity factor K of the profile is larger than the critical value K_{cr} of the material cracks do propagate.

For the array of edge cracks loaded by an uniaxial remote stress, the stress intensity factor is given in closed form (Tada et al., 1985) as

$$K_I = \sigma_\infty\sqrt{\frac{\lambda}{2}} \quad \text{or in dimensionless form} \quad \frac{K_I}{\sigma_\infty\sqrt{\pi a}} = \sqrt{\frac{1}{2\pi}\frac{\lambda}{a}} \tag{29}$$

where a is the crack length which has to be sufficiently larger than λ ('well developed cracks').

Noda and Tsuru (1996) estimated numerically the variation of K_I for an array of surface cracks with the ratio a/λ, obtaining the results reported in the second line of the following Table 1, where a comparison with the theoretical solution (29) is also presented.

For a going to zero, the classical value of the isolated edge crack under remote tension is recovered $K_I/\sigma_\infty\sqrt{\pi a} = 1.1215$, whilst as a/λ increases the influence of a gets smaller and smaller since the numerical solution tends to the theoretical value of (29), as shown in Table 1 and Fig. 4. For $a/\lambda \simeq 0.2$, the percentage difference between the two solutions is smaller than 3%, thus 'well developed cracks' are those with $a > 0.2\lambda$. Consequently, the analytical solution (29) can be used as a conservative estimation of the likelihood of cracks to propagate.

Table 1
Numerical and analytical stress intensity factors for an array of edge cracks as from Fig. 1a

a/λ	0.0	0.1	0.2	0.3	0.4	0.5
$K_I/\sigma_\infty\sqrt{\pi a}$ (N&D)	1.1215	1.039	0.872	0.727	0.627	0.560
$K_I/\sigma_\infty\sqrt{\pi a}$ (analytical)	∞	1.261	0.892	0.728	0.630	0.564

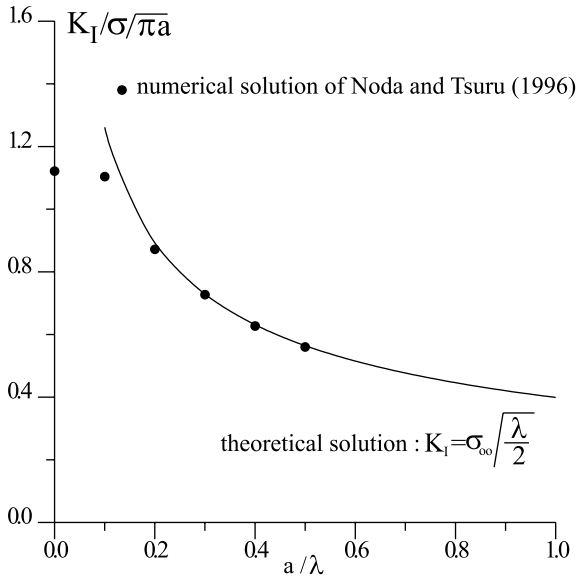

Fig. 4. A comparison between the numerical and theoretical stress intensity factors $K_I/\sigma\sqrt{\pi a}$ for an array of edge cracks under remote tension as a function of the ratio a/λ between the crack depth a and spacing λ.

If a fragile material is considered, that is neglecting the nucleation of any dislocations, the critical conditions for crack propagation are reached when the energy release rate Γ equals two times the surface energy γ ($\Gamma_{cr} = 2\gamma$). Under plane strain conditions, the energy release rate is $\Gamma = (1-\nu^2)K_I^2/E$. Therefore, combining the above formulae it follows

$$K_{I\,cr} = \sqrt{\frac{2\gamma E}{(1-\nu^2)}} \tag{30}$$

Noticing that the array of edge cracks is unstable if $K > K_{I\,cr}$, from (29) and (30), the critical remote stress σ_{cr}^{SC} for supercritical propagation of the array of cracks is derived as

$$\sigma_{cr}^{SC} \geqslant \sqrt{\frac{4\gamma E}{(1-\nu^2)\lambda}} \tag{31}$$

at fixed spacing λ; whilst the critical wavelength λ_{cr}^{SC} above which the array of cracks propagates supercritically for a fixed remote load

$$\lambda_{cr}^{SC} \geqslant \frac{1}{\sigma_\infty^2}\frac{4\gamma E}{(1-\nu^2)} \tag{32}$$

Substituting for the parameter β and normalizing the remote stress σ_∞, it follows

$$\breve{\sigma}_{cr}^{SC} = \sqrt{\frac{4\beta}{\pi\lambda}} \quad \text{and} \quad \lambda_{cr}^{SC} = \frac{4\beta}{\pi\breve{\sigma}_\infty^2} \tag{33}$$

Notice that rephrasing $\breve{\sigma}_{cr}^{SC}$ in dimensional form and rearranging, it derives

$$\Lambda = \left(\frac{\sigma_\infty^2\lambda}{\gamma E/(1-\nu^2)}\right) = 4 \tag{34}$$

which coincides with (2) for $\gamma_B = 0$ and plane strain. Therefore, the critical conditions for the supercritical propagation of a crack-like surface can be easily estimated using linear fracture mechanics, avoiding unnecessarily complicated long-term analysis.

4. Discussions

In the previous sections the critical conditions for the onset of stress-induced MI and supercritical propagation of an array of edge cracks have been addressed in terms of limiting loads and wavelengths (or wave numbers). In the sequel, these two limiting conditions are compared with the aim of understanding if and under which situations MI could lead to SC. Again two different conditions are considered: fixed wavelength $\lambda = 2\pi/m$ (Case I), and arbitrary rough surface with a fixed remote stress σ_∞ (Case II). The diagrams reported in the sequel have been determined for the material properties typical of Si amorphous–crystal transition (Table 2), as from Voorhess and Aziz (2000), for which $\alpha = 4.0 \times 10^{-3}$ and $\beta = 10^{-11}$ (m).

4.1. Case I: Fixed wavelength $\lambda = 2\pi/m$

This case is typical of polycrystalline solids, such as ceramic coatings, or micropatterned surfaces widely used in biomedical applications. The critical loading conditions are presented in (23) for both a tensile remote stress (σ_{1cr}) and a compressive remote stress (σ_{2cr}), and these two relations are plotted in Fig. 5, for $\alpha = 4.0 \times 10^{-3}$ and $\beta = 10^{-11}$ (m). A log–log diagram is used, thus for compressive loading the modulus of the remote stress is plotted. The area above the two curves is the critical zone, whilst below the curves the system is stable. The critical stresses reduces as the wavelength of the perturbation increases tending to a small frequency limit ($\lambda \to \infty$) given by

$$\lim_{\lambda\to\infty} \breve{\sigma}_{1cr} = 2\alpha; \quad \lim_{\lambda\to\infty} \breve{\sigma}_{2cr} = 0 \tag{35}$$

Consequently, under tensile load there exists an absolute threshold load below which no MI occurs, and for the material properties given in Table 2 this threshold load is equal to 0.8 GPa. Conversely, for a compressive load such a threshold limit is zero, that is to say there is no threshold limit.

Moreover, it must be noticed that in real applications perturbations with wavelengths smaller or at most equal to the maximum geometric extension L of the surface can be supported, therefore from (23) a relative threshold load can be defined for both compressive and tensile remote loading as

Table 2
Material properties for Si microelectronic components

E (GPa)	ν	F_0 (J m^{-3})	γ (J m^{-2})	Ω (m^3)	T (K)	V^* (m^3)
75	0.25	6.27×10^8	0.4	10^{-30}	793	0.14Ω

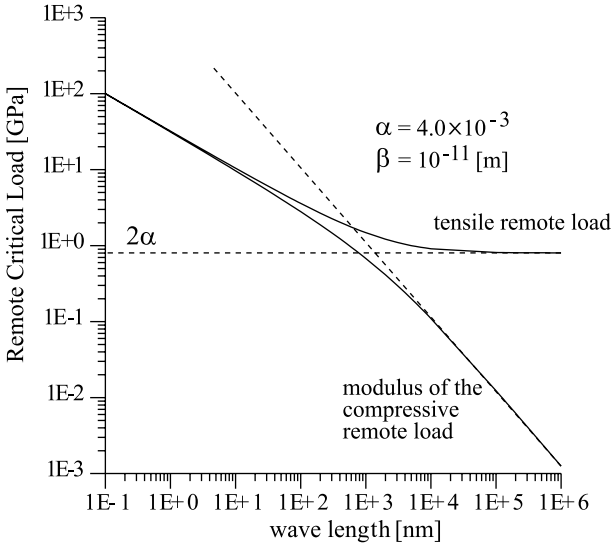

Fig. 5. The tensile and compressive critical loads σ_∞ (GPa) as a function of the wavelength λ (nm) ($\alpha = 4.0 \times 10^{-3}$; $\beta = 10^{-11}$ m).

Table 3
Threshold stress for MI as a function of the characteristic geometric dimension L, for Si in microelectronic components

L	1 nm	1 μm	1 mm	1 m
σ_{1th}	10.5 GPa	0.90 GPa	0.8 GPa	0.8 GPa
σ_{2th}	−9.6 GPa	−0.11 GPa	−0.12 MPa	−0.12 kPa

$$\breve{\sigma}_{1\mathrm{th}} = \alpha + \sqrt{\alpha^2 + \frac{\beta}{L}} \quad \text{and} \quad \breve{\sigma}_{2\mathrm{th}} = \alpha - \sqrt{\alpha^2 + \frac{\beta}{L}} \tag{36}$$

which takes up the values listed in Table 3.

Notice that in the micrometer range, typical of microelectronic applications, the threshold stresses for Si can be much smaller than commonly measured mismatch stresses (order of 1 GPa).

Consider the tensile remote stress, the sole that could be critical for the unstable propagation of an array of edge cracks. If the critical remote stress for the onset of MI $\breve{\sigma}_{\mathrm{cr}}^{\mathrm{MI}}$ and that for the supercritical propagation of an array of edge cracks $\breve{\sigma}_{\mathrm{cr}}^{\mathrm{SC}}$ are compared a characteristic wavelength can be deduced λ_{tr}, that can be called *transitional wavelength*, above which $\breve{\sigma}_{\mathrm{cr}}^{\mathrm{MI}}$ is always larger than $\breve{\sigma}_{\mathrm{cr}}^{\mathrm{SC}}$, that is

$$\begin{aligned} &\lambda < \lambda_{\mathrm{tr}} : \breve{\sigma}_{\mathrm{cr}}^{\mathrm{MI}} < \breve{\sigma}_{\mathrm{cr}}^{\mathrm{SC}} \\ &\lambda = \lambda_{\mathrm{tr}} : \breve{\sigma}_{\mathrm{cr}}^{\mathrm{MI}} = \breve{\sigma}_{\mathrm{cr}}^{\mathrm{SC}} \\ &\lambda > \lambda_{\mathrm{tr}} : \breve{\sigma}_{\mathrm{cr}}^{\mathrm{MI}} > \breve{\sigma}_{\mathrm{cr}}^{\mathrm{SC}} \end{aligned} \tag{37}$$

Therefore only for $\lambda > \lambda_{\mathrm{tr}}$ the stress-induced MI could lead to catastrophic failure by supercritical crack propagation, given enough time for a crack-like surface to form. The transitional wavelength is readily determined solving the equation $\breve{\sigma}_{\mathrm{cr}}^{\mathrm{SC}} = \breve{\sigma}_{\mathrm{cr}}^{\mathrm{MI}}$ for λ, thus

$$\lambda_{\mathrm{tr}} = \frac{1}{\pi}\left(\frac{\pi}{4} - 1\right)^2 \frac{\beta}{\alpha^2} \tag{38}$$

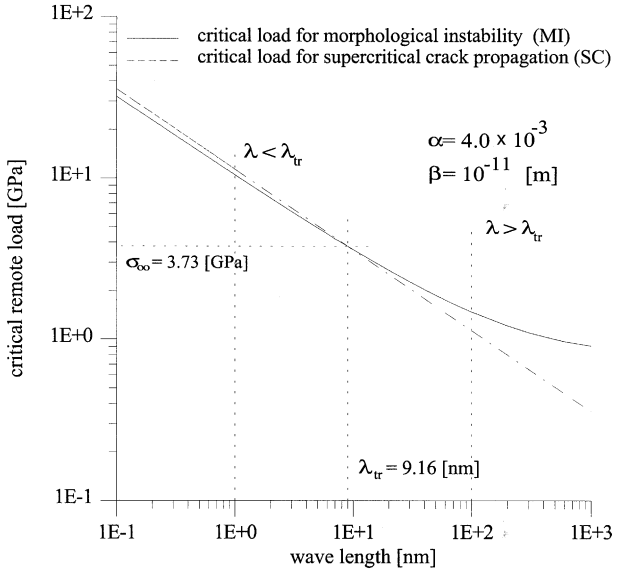

Fig. 6. Case I—fixed wavelength $\lambda = 2\pi/m$: a comparison between the critical conditions for the onset of MI (—) and the critical conditions for the supercritical propagation of an array of edge cracks (- - -). The two curves intersect at the transitional wavelength λ_{tr}.

In Fig. 6, the dimensionless critical loads for the onset of MI and for the onset of SC are plotted against the wavelength λ using the material properties listed in Table 2. With this data the transitional wavelength is $\lambda_{tr} = 9.16$ nm and the corresponding critical stress for MI $\sigma_{cr}^{MI} = 3.73$ GPa. Notice that if the kinetically driven instability is neglected, that is to say $V^* = \alpha = 0$, the transitional wavelength would be infinitely large meaning that energetically driven MI could never lead to catastrophic failure. In fact under these conditions the critical load for the onset of MI is $\breve{\sigma}_{cr}^{MI} = \sqrt{\beta/\lambda}$ which is always smaller than $\sigma_{cr}^{SC} = \sqrt{4\beta/(\pi\lambda)}$: MI could only lead to a stable crack-like surface. Notice that the case $\breve{\sigma}_{cr}^{MI} = \sqrt{\beta/\lambda}$ corresponds to $\Lambda = \pi$ of Yu and Suo (1999).

It is also interesting to estimate the percentage difference Δ between the two critical loads as λ varies, which is readily given by

$$\Delta(\lambda) = \frac{\sigma_{cr}^{SC} - \sigma_{cr}^{MI}}{\sigma_{cr}^{MI}} \times 100 = \left(\frac{\frac{2}{\sqrt{\pi}}\sqrt{\frac{\beta}{\lambda}}}{\alpha + \sqrt{\alpha^2 + \frac{\beta}{\lambda}}} - 1 \right) \times 100 \tag{39}$$

For $\lambda < \lambda_{tr}$, the difference Δ is positive and grows with λ from $\Delta(\lambda = \lambda_{tr}) = 0$ to $\Delta(\lambda \to 0) = \left(\sqrt{4/\pi} - 1\right) \times 100 \simeq 13\%$, showing that the maximum difference between σ_{cr}^{SC} and σ_{cr}^{MI} is of about 13%, negligible in most cases. However, in practice, dislocations may nucleate at the flaw tip, thus increasing the load needed for crack supercritical propagation and the percentage difference $\Delta(\lambda)$. This could be taken into account by summing up at the surface tension γ the term $\gamma_p > 0$, thus increasing the surface energy of the system at the flaw tip.

4.2. Case II: Arbitrary rough surface with a fixed remote load σ_∞

Consider a rough surface where perturbations of various wavelength coexist. In this case the remote stress is fixed and the independent variable affecting the solution is the wavelength λ. In a previous section,

the critical wavelengths for both the onset of MI λ_{cr}^{MI} (26) and supercritical propagation of an array of edge cracks λ_{cr}^{SC} (33) have been presented as a function of the material parameters α and β. In addition it has been pointed out that a dominant perturbation exists for the onset of MI and it is given by $\lambda_{max} = 2\lambda_{cr}^{MI}$. Noticing that among all the components, eventually the sole dominant perturbation would evolve towards a crack-like profile, a comparison between λ_{cr}^{SC} and λ_{max} is performed. Thus, for a fixed tensile load, it follows that

$$\lambda_{max} = \frac{2\beta}{\breve{\sigma}_\infty\left(\breve{\sigma}_\infty - 2\alpha\right)} \lessgtr \frac{2}{\pi}\frac{2\beta}{\breve{\sigma}_\infty^2} = \lambda_{cr}^{SC} \tag{40}$$

where the sign of the above equation is defined by the sign of α, that is

$$\alpha < 0 : \lambda_{max} \lessgtr \lambda_{cr}^{SC} \quad \text{if } \breve{\sigma}_\infty \lessgtr \frac{4}{(\pi - 2)}|\alpha|$$

$$\alpha = 0 : \lambda_{max} > \lambda_{cr}^{SC} \quad \text{being } \frac{2}{\pi} < 1$$

$$\alpha > 0 : \lambda_{max} > \lambda_{cr}^{SC} \quad \text{being } \breve{\sigma}_\infty > 2\alpha^2$$

Recalling that wavelengths larger than λ_{cr}^{SC} are critical against crack propagation, MI would always lead to catastrophic failure for $\alpha \geqslant 0$. On the other hand, for $\alpha < 0$, catastrophic failure would be induced only for $\breve{\sigma}_\infty > 4|\alpha|/(\pi - 2) \approx 3.5|\alpha|$. These results are plotted in Fig. 7, for the material properties of Table 2.

4.3. The effect of the material parameters α and β

For a fixed λ, the criticalness of the system is assessed by the transitional wavelength λ_{tr} and it depends on the material parameters α and β. Conversely, for an arbitrary rough surface with a fixed remote load, catastrophic failure occurs if and only if $\breve{\sigma}_\infty < (4/(\pi - 2))|\alpha|$ (for $\alpha < 0$), which depends on the sole para-

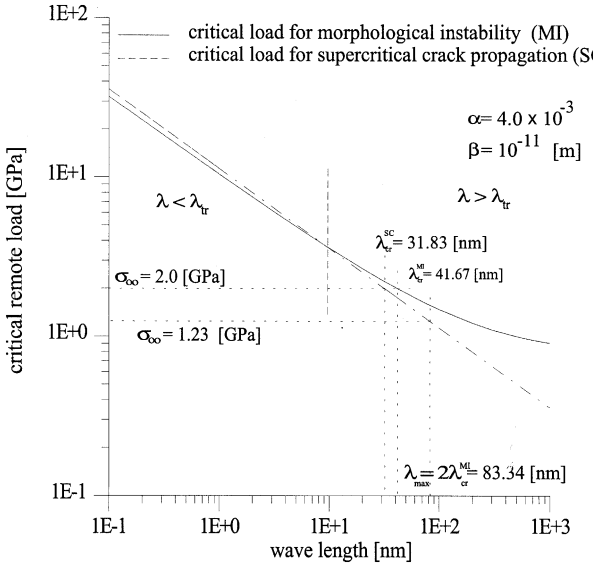

Fig. 7. Case II—fixed remote load σ_∞: a comparison between the critical conditions for the onset of MI (—) and the critical conditions for the supercritical propagation of an array of edge cracks (- - -). The dominant perturbation $\lambda_{max} = 2\lambda_{cr}^{MI}$ has a wavelength larger than the critical perturbation for the supercritical propagation of an array of edge cracks λ_{cr}^{SC}.

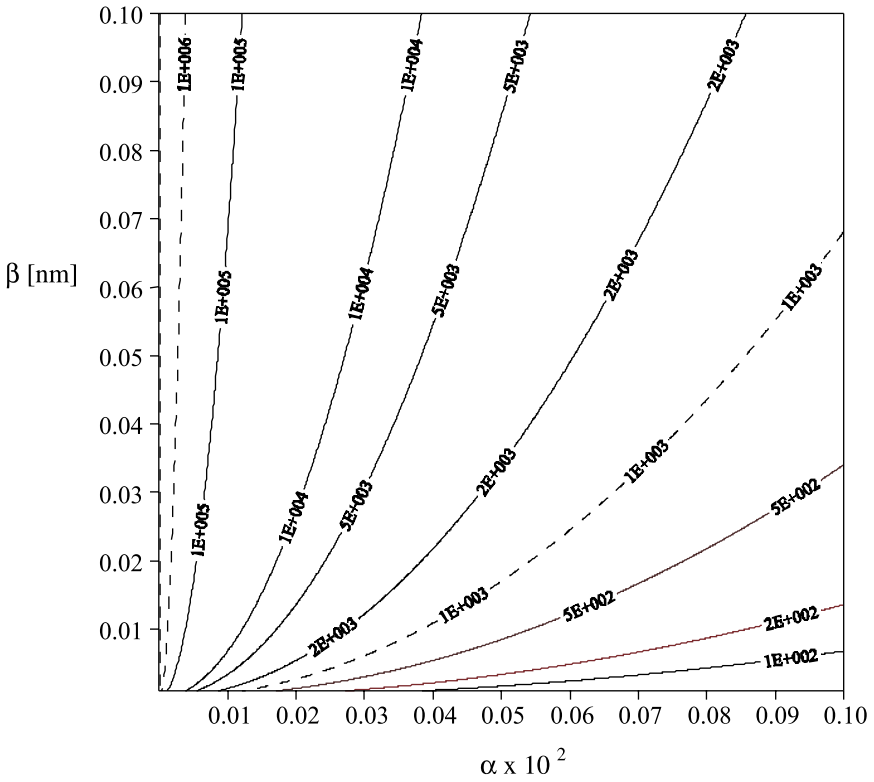

Fig. 8. The influence of the material parameters α and β on the transitional wavelength λ_{tr}: the larger is α and the smaller is β more likely is the occurring of catastrophic failure related to stress-driven MI.

meter α. As a consequence, it is interesting to study the influence of the material parameters α and β on the transitional wavelength λ_{tr}.

Usually, the parameter β takes up small positive values being the Young's modulus E much larger than the surface tension γ

$$\beta = \frac{\pi(1-\nu)}{(1+\nu)}\frac{\gamma}{E} \quad \text{say} = 10^{-3}\text{–}10^{-1}\ (\text{nm}) \tag{41}$$

whilst the parameter α can take up positive and negative values depending on the sign of V^*

$$\alpha = \tanh\left[\frac{F_0\Omega}{2kT}\right]\frac{V^*}{\Omega} \quad \text{say} = 0\text{–}0.01 \tag{42}$$

In Fig. 8, the log–log contour plots of the transitional wavelength λ_{tr} is plotted against the parameters α and β

$$\lambda_{tr} = \exp\left[\log\left[\frac{1}{\pi}\left(\frac{\pi}{4}-1\right)^2\right] + \log\beta - 2\log\alpha\right] \tag{43}$$

It is worth recalling that as the transitional wavelength λ_{tr} increases, the likelihood that MI could induce SC decreases. As the parameter α grows the transitional wavelength decreases rapidly, whilst the parameter β has an opposite influence on λ_{tr}.

5. Conclusions

Stress-driven MI has been studied by means of a small perturbation technique. The dependence of the atomic mobility M on the stress field has been considered in the kinetic law in order to examine both the classical energetically driven instability and the more recently introduced kinetically driven instability. The stability of the system has been assessed investigating the stability of atomic motion regardless of the transport mechanism (surface diffusion, evaporation and condensation, chemical reactions), thus leading to a more intuitive and straightforward derivation of a general stability condition. By means of a classical small perturbation analysis the critical remote loads $\sigma_{\mathrm{MI}}^{\mathrm{cr}}$ and wavelengths $\lambda_{\mathrm{MI}}^{\mathrm{cr}}$ for the onset of MI have been defined as a function of the material parameters α and β. In fact, by normalizing the stability equation two governing material parameters have been identified: $\alpha\ (= V^*/\Omega \times \tanh[F_0\Omega/2kT])$, which is dimensionless and related to the driving force F_0 and activation strain V^*, and $\beta\ (= \pi(1-\nu)/(1+\nu) \times \gamma/E)$, having the dimension of a length and being proportional to the ratio γ/E. Moreover, observing that MI could evolve into crack-like surfaces, the critical conditions for the supercritical propagation of an array of edge cracks (SC) has been determined in terms of limiting loads $\sigma_{\mathrm{cr}}^{\mathrm{SC}}$ and wavelengths $\lambda_{\mathrm{cr}}^{\mathrm{SC}}$. Finally, the two sets of critical conditions for MI and SC have been compared with the aim of defining if and under which situations MI could lead to catastrophic failure of microdevices by supercritical crack propagation.

Two different practical cases have been considered: (i) a fixed wavelength $\lambda = 2\pi/m$ (Case I), typical for polycrystalline materials and micropatterned surfaces; (ii) arbitrary rough surface with a fixed remote load σ_∞ (Case II).

The following results have been obtained:

Case I—fixed wavelength:

1. The stability condition depends on both material parameters α and β.
2. Two different threshold loads (compressive and tensile) for the onset of MI have been introduced as a function of material parameters α and β, as from (23). Also, for $\alpha > 0$, it has been shown that MI could never occur if $\breve{\sigma}_{1\mathrm{cr}} < 2\alpha$, whilst no threshold load exists under compression ($\breve{\sigma}_{2\mathrm{cr}} = 0$).
3. The effects of a finite size domain L on the stability prediction has been incorporated (Eq. (36)), showing that in the micrometer range threshold loads could be much smaller than typical mismatch stresses (order of 1 GPa), and demonstrating again that MI is very likely.
4. A transitional wavelength λ_{tr} has been introduced, as a function of the material parameters α and β, above which MI could always lead to SC and failure, given enough time for the surface to evolve.
5. For $\alpha = 0$, i.e. energetically driven MI would never lead to SC being $\breve{\sigma}_{\mathrm{cr}}^{MI} < \breve{\sigma}_{\mathrm{cr}}^{\mathrm{SC}}$.

Case II—arbitrary rough surface with a fixed remote load:

1. The stability condition depends on the sole material parameters α.
2. It has been found that the wavelength of the dominant perturbation, that is the perturbation with the largest growth rate, which eventually would degenerate into a crack-like surface, is always larger than $\lambda_{\mathrm{cr}}^{\mathrm{SC}}$ the critical wavelength for SC for $\alpha \geqslant 0$, meaning that MI would always lead to SC given enough time for the surface to evolve.

Finally, it has been investigated the influence of the material properties α and β on such limiting conditions, showing that the transitional wavelength reduces, that is to say catastrophic failure due to MI is more likely, as the driving force F_0, the activation energy V^* and the surface tension γ increase, and the Young's modulus E reduces.

References

Asaro, R.J., Tiller, W.A., 1972. Interface morphology development during stress corrosion cracking. Part 1. Via surface diffusion. Metallurgical Transactions 3, 1789–1796.

Aziz, M.J., Sabin, P.C., Lu, G.-Q., 1991. The activation strain tensor: non-hydrostatic stress effect on crystal-growth kinetics. Physical Review B 44 (18), 9812–9816.

Barvosa-Carter, W., Aziz, M.J., Cray, L.J., Kaplan, T., 1998. Kinetically driven growth instability in stressed solids. Physical Review Letters 81 (7), 1445–1448.

Chiu, C.-H., Gao, H., 1993. Stress singularities along a cycloid rough surface. International Journal of Solids and Structures 30 (21), 2983–3012.

Chiu, C.-H., Gao, H., 1994. Numerical simulation of diffusion controlled surface evolution. Materials Research Symposium Proceedings 317, 369–374.

Freund, L.B., 1995. Evolution of waviness on the surface of a strained elastic solid due to stress-driven diffusion. International Journal of Solids and Structures 32 (6/7), 911–923.

Noda, N.-a., Tsuru, M., 1996. Stress intensity factors of double and multiple edge cracks. Transactions of the Japanese Society for Mechanical Engineering 62 (598), 1362–1367.

Ohring, M., 1992. The Material Science of Thin Films. Academic Press, Inc.

Srolovitz, D.J., 1989. On the stability of surfaces of stressed solids. Acta Metallurgica 37 (2), 621–625.

Tada, H., Paris, P.C., Irwin, G.R., 1985. The Stress Analysis of Cracks Handbook. Dell Research Corporation, Hellertown, PA.

Voorhess, P.W., Aziz, M.J., 2000. The effect of a stress-dependent mobility on interfacial stability, submitted for publication.

Yang, W.H., Srolovitz, D.J., 1993. Crack-like surface instabilities in stressed solids. Physical Review Letters 71 (10), 1593–1596.

Yu, H.H., Suo, Z., 1999. Delayed fracture of ceramics caused by stress-dependent surface reactions. Acta Materialia 47 (1), 77–88.

Yu, H.H., Suo, Z., 2000. Stress-dependent surface reactions and implications for a stress measurement technique. Journal of Applied Physics 83 (3), 1211–1218.